Chinese Chemical Letters 31 (2020) 181–184

Contents lists available at ScienceDirect

Chinese Chemical Letters

journal homepage: www.elsevier.com/locate/cclet

Communication

Synthesis of core-shell structured Au@Bi_2S_3 nanorod and its application as DNA immobilization matrix for electrochemical biosensor construction

Feng Gao[a,c,*], Juan Song[a], Bin Zhang[a], Hidekazu Tanaka[b], Fei Gao[a], Weiwei Qiu[a,b], Qingxiang Wang[a]

[a] Department of Chemistry and Environment Science, Minnan Normal University, Zhangzhou 363000, China
[b] Department of Chemistry, Graduate School of Science and Engineering, Shimane University, Matsue, Shimane 690-8504, Japan
[c] Key Laboratory of Sensor Analysis of Tumor Marker Ministry of Education, College of Chemistry and Molecular Engineering, Qingdao University of Science and Technology, Qingdao 266042, China

ARTICLE INFO

Article history:
Received 2 March 2019
Received in revised form 18 April 2019
Accepted 18 April 2019
Available online 19 April 2019

Keywords:
DNA biosensor
Au@Bi_2S_3 nanorods
Electrochemical impedance spectroscopy
Core-shell structure
Bi^{3+}-N bond
Probe immobilization

ABSTRACT

The core-shell structured Au@Bi_2S_3 nanorods have been prepared through direct *in-situ* growth of Bi_2S_3 at the surface of pre-synthesized gold nanorods. The product was characterized by X-ray diffraction, transmission electron microscopy and energy-dispersive X-ray spectroscopy. Then the obtained Au@Bi_2S_3 nanorods were coated onto glassy carbon electrode to act as a scaffold for fabrication of electrochemical DNA biosensor on the basis of the coordination of $-NH_2$ modified on 5′-end of probe DNA and Au@Bi_2S_3. Electrochemical characterization assays demonstrate that the Au@Bi_2S_3 nanorods behave as an excellent electronic transport channel to promote the electron transfer kinetics and increase the effective surface area by their nanosize effect. The hybridization experiments reveal that the Au@Bi_2S_3 matrix-based DNA biosensor is capable of recognizing complementary DNA over a wide concentration ranging from 10 fmol/L to 1 nmol/L. The limit of detection was estimated to be 2 fmol/L (S/N = 3). The biosensor also presents remarkable selectivity to distinguish fully complementary sequences from base-mismatched and non-complementary ones, showing great promising in practical application.
© 2019 Chinese Chemical Society and Institute of Materia Medica, Chinese Academy of Medical Sciences. Published by Elsevier B.V. All rights reserved.

Take advantages of its narrow band gap (1.2–1.7 eV), outstanding energy conversion efficiency and high absorption coefficient (10^4–10^5 cm^{-1}), bismuth sulfide (Bi_2S_3) receives great attention in the application of electrochemical field [1,2]. In addition, with the development of material science and nanotechnology, the nano-sized Bi_2S_3 with various morphologies have been synthesized and utilized as high-performance electrochemical sensing materials [3–5]. For example, Dong and coworkers [3] have constructed a nanorod Bi_2S_3-based electrochemical sensor for ascorbic acid analysis, achieving high sensitivity and excellent reliability. Fu [4] synthesized three-dimensional Bi_2S_3 nanowire network, and utilized the prepared Bi_2S_3 nanowire network to construct an electrochemical ammonia sensor. The result showed that the sensor had an excellent specific response to ammonia due to their weak coordination adsorption action. Our group [5] also synthesized a unique broccoli-like Bi_2S_3 using an imidazoline derivative as the template and investigated its electrocatalysis toward the bovine hemoglobin. The results showed that the Bi_2S_3 could effectively promote the direct electrochemistry of hemoglobin, and the prepared electrode displayed excellent electrocatalysis of hydrogen peroxide as an enzyme biosensor.

However, the pure Bi_2S_3 nanomaterial is easily aggregated during the synthesis process, which not only decreases its effective surface area, but also weakens the electrochemical properties [6]. On the purpose of getting around these shortcomings, the other functional materials such as carbon material [7,8], polymers [9], and precious metals [10,11] are usually introduced as supporting material or auxiliary material for the synthesis of the Bi_2S_3-based nanocomposites.

Gold nanoparticles (AuNPs) are an important and widely used precious metal nanomaterial bearing lots of excellent physicochemical properties such as good biocompatibility, high electronic conductivity, and outstanding adhesive ability with organic groups including —NH_2, —SH, and so forth [12–15]. Based on these features, AuNPs are frequently utilized as a scaffold for bioprobe

* Corresponding author at: Department of Chemistry and Environment Science, Minnan Normal University, Zhangzhou, 363000, China.
E-mail address: fgao1981@126.com (F. Gao).

https://doi.org/10.1016/j.cclet.2019.04.056
1001-8417/© 2019 Chinese Chemical Society and Institute of Materia Medica, Chinese Academy of Medical Sciences. Published by Elsevier B.V. All rights reserved.

immobilization [16,17] and electrochemical signal amplifier [18,19]. In recent years, the AuNPs have also been utilized as functional material to prepare Bi_2S_3-based composite, and be extended to the application in the field of electrochemistry. For example, Zhang *et al.* [20] synthesized AuNPs/Bi_2S_3 nanorods and applied them as signal tags to catalyze silver deposition. Through such a strategy, an ultrasensitive electrochemical immunosensor for *Escherichia Co*1:*O*157:*H*7 was achieved using silver stripping signal as the analytical signal. In addition, Li *et al.* [21] have synthesized a new composite of $KNbO_3$-AuNPs@Bi_2S_3, and used the composite as an antibody carrier for the analysis of prostate-specific antigen. The result showed that the AuNPs/Bi_2S_3 connected by Au-S covalent bond could effectively promote electron transfer kinetics and electrochemiluminescence signal intensity. However, we have not found the report concerning the use of AuNP/Bi_2S_3 composite as a matrix for probe DNA immobilization and electrochemical sensing analysis yet.

Herein, a rod-like core-shell structured Au@Bi_2S_3 composite was designed and prepared through direct growth of Bi_2S_3 shell on pre-synthesized gold nanorods. The sample was characterized by X-ray diffraction (XRD), transmission electron microscopy (TEM) and energy-dispersive X-ray spectroscopy (EDS). Electrochemical characterization experiment suggested that the gold core could dramatically decrease the electron transfer resistance of Bi_2S_3. Furthermore, the Au@Bi_2S_3 coated glassy carbon electrode (GCE) was utilized as a scaffold for the self-assembly fixing of the amino-modified oligonucleotide probe to fabricate an electrochemical DNA biosensor. Under the optimized conditions, the target DNA could be well detected with a low detection limit of femtomolar level (2 fmol/L). This work broadens the application of Au and Bi_2S_3 nanocomposite in electrochemical sensing fields, and provides a new method for facile construction of a sensitive biosensor.

Firstly the gold nanorods were synthesized according to Ag^+-assisted seed-mediated approach [22] with minor modification (Scheme 1A). Typically, an aliquot of 5.0 mL 0.02 mmol/L $HAuCl_4$ solution was mixed first with 5.0 mL 200 mmol/L CTAB. Then 0.6 mL of ice-cold $NaBH_4$ (10 mmol/L) was prepared and dropped into above mixture under vigorous stirring. During this process, the solution was transformed from dark-yellow to brown-yellow, which is a characteristic of formation of the gold seed in the solution. Followed by, put the gold seed solution into a water bath (25 °C) for more than 2 h to decompose the unreacted $NaBH_4$.

What is more, the mixture of 75.0 mL of 200 mmol/L cetyltrimethylammonium bromide (CTAB), 75.0 mL of 1 mmol/L $HAuCl_4$, 1.25 mL of 4 mmol/L $AgNO_3$ and 1.05 mL of 100 mmol/L L-ascorbic acid was prepared and continuously stirred, which was acted as the gold nanorods growth solution. Thereafter, 180 μL prepared gold seed solution was added into the freshly prepared growth solution, and kept the reaction temperature at 25 °C. In 15 min, the color of the reaction solution became dark red, suggesting the reduction of Au^{3+} to Au^0 species. After further grown for 24 h in the mixture solution, the gold nanorods (AuNR) were collected by centrifugation at 8000 rpm for 15 min, and finally, the gold nanorods dispersion was obtained by suspending the synthesized Au nanorods in 20.0 mmol/L CTAB.

Core-shell structured Au@Bi_2S_3 AuNR were prepared through direct growth of Bi_2S_3 on the surface of AuNR (Scheme 1B). In detail, 3.0 mL 0.1 mol/L Na_2S was added into 30 mL of above-prepared AuNR dispersion in a vessel open to the air with vigorous stirring at room temperature. The mixture was aged for 1 h in water bath at 50 °C. The particles were then collected by centrifugation and then dispersed in 20.0 mmol/L CTAB. Thereafter, 4.5 mL of 0.1 mol/L $Bi(NO_3)_3$ was added into the solution and reacted with S^{2-} capped gold nanorods in a 60 °C water bath for 1 h to grow Bi_2S_3 on the surface of AuNR. Finally, the formed Au@Bi_2S_3 nanorods

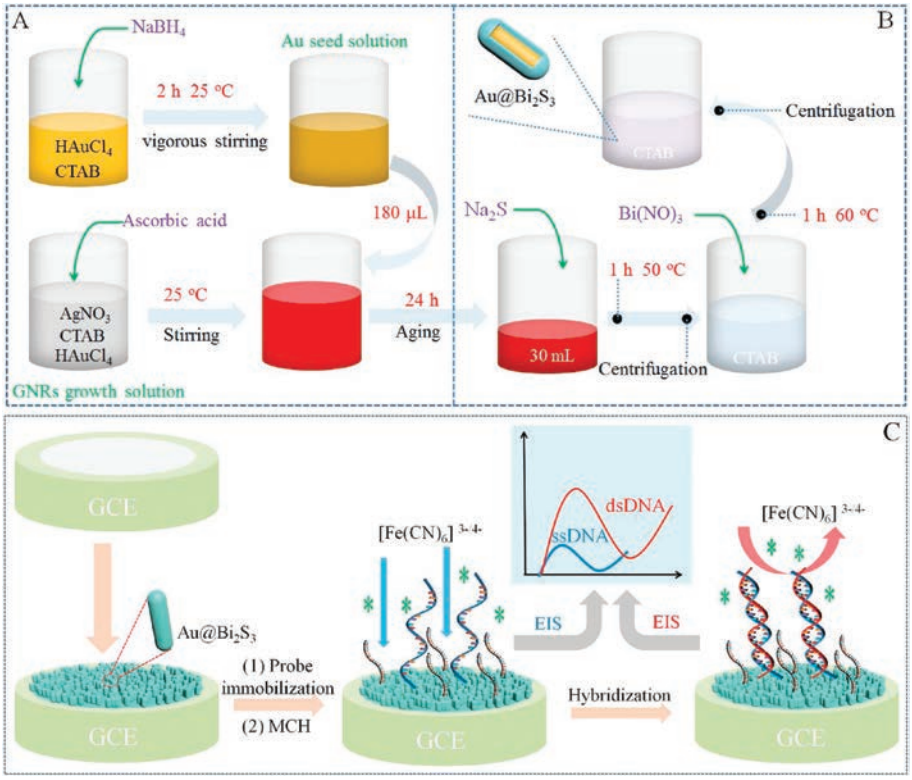

Scheme 1. Schematic diagram for preparation of gold nanorods (A) and the core-shell structured Au@Bi_2S_3 (B). (C) The fabrication process of the Au@Bi_2S_3-based DNA electrochemical biosensor and its analytical application.

were obtained through centrifugation. The stock solution of the Au@Bi_2S_3 was prepared by dispersing 1 mg Au@Bi_2S_3 sample in 10 mL 20.0 mmol/L CTAB.

The biosensor was fabricated as following procedure: First, 10 μL prepared Au@Bi_2S_3 dispersion was dropped onto a GCE pretreated through physical polishing with alumina slurry, and electrochemically polishing *via* a CV process in 0.5 mol/L H_2SO_4, as described in the literature [23]. Then 10 μL of the prepared Au@Bi_2S_3 dispersion was dropped onto the surface of the pretreated GCE and dried under room temperature. Afterward, the loosely attached Au@Bi_2S_3 on the electrode was removed by gentle rinsing with DDW for three times, and the obtained electrode was signed as Au@Bi_2S_3/GCE. It is of note that, the bare GCE after electrochemical treatment in H_2SO_4, bears some functional oxygen-containing groups, which is beneficial for assembly of Au@Bi_2S_3 through tight coordination and electrostatic interaction with surface Bi^{3+} of the material. Thus, the stability of the modified electrode is ensured. To further assemble the amino group modified pDNA (5′-NH_2-TCTTTGGGACCACTGTCG-3′) on electrode through coordination between $-NH_2$ and Bi_2S_3 [24], the Au@Bi_2S_3/GCE was immersed in 0.1 μmol/L pDNA for 4 h at 30 °C. Then the electrode was incubated in 1 mmol/L 6-mercapto-1-hexanol (MCH) for 2 h to passivate the residual sites between the DNA probes. Finally, the electrode was rinsed with phosphate buffer saline (PBS) to removed physically attached pDNA, and the biosensor (pDNA/Au@Bi_2S_3/GCE) was achieved. For comparison, the Bi_2S_3/GCE was also fabricated through a similar procedure only replacing single phase Bi_2S_3 with Au@Bi_2S_3. All the detailed reagents and apparatus were listed in Supporting information.

The composition and structure of the synthesized composite were characterized by XRD. As displayed in Fig. 1A, the diffraction peaks and the corresponding crystal planes for Au nanorod precursor, $2\theta = 38.75°$ (111), 39.8° (200), 64.92° (220) and 77.50° (311) are well consistent with the results of nano gold PDF# 89–3697, proving the successful synthesis of the gold nanorods through the Ag^+-assisted seed-mediated method. In addition, the XRD pattern of CTAB (PDF#48-2454) is appeared in AuNR, suggesting that CTAB is adsorbed on the surface of AuNR during the synthesis process. The presence of CTAB can well prevent the aggregation of AuNR. For Au@Bi_2S_3, it is found that all the characteristic diffraction peaks of Au are visible but their intensity is much weaker than the pure AuNR, which is likely caused by the coating of Bi_2S_3 shell. In addition, one can clearly observe the diffraction peaks ascribing to Bi_2S_3 at $2\theta = 15.67°$ (002), 17.58° (012), 25.0° (111), 28.6° (121), 40.0° (034), 45.5° (200), 52.6° (213), 57.4° (241), confirming that Bi_2S_3 has successfully grown on AuNR.

Then, the obtained products were characterized by TEM. As displayed in Fig. 1B, the Au@Bi_2S_3 particles show uniform rod shape with the average length of 58 nm, diameter of 20 nm, and draw ratio of 6:1. Fig. 1C is the HRTEM image of Au@Bi_2S_3, from which one can see that the distance between the crystal planes in the middle of the nanorod is 0.237 nm, corresponding to cubic phase of Au crystal (111) lattice face [25]. The distance between the crystal planes at the shell of the nanorod is 0.205 nm, which belongs to the orthorhombic phase of Bi_2S_3 crystal (002) lattice facet. This result further testifies that the Au@Bi_2S_3 composite has a core-shell structure. The EDS (Fig. 1D) analysis demonstrates that the particles are comprised by the elements of Au (9.71 keV), S (2.31 keV) and Bi (10.84 keV), further confirming the successful synthesis of Au@Bi_2S_3 by the proposed method.

The electrochemical property of Au@Bi_2S_3 and the fabrication of pDNA/Au@Bi_2S_3/GCE were characterized by cyclic voltammetry (CV) and electrochemical impedance spectra (EIS) (Fig. S1 in Supporting information). Both of the results suggest successful fabrication of the biosensor. Under the optimized conditions (Fig. S2 in Supporting information), the analytical performance of the biosensor is evaluated by EIS since it is a simple and effective approach for electrode characterization and biosensing analysis [26]. Fig. 2A shows the R_{et} value difference (ΔR_{et}) on the biosensor before (curve a) and after hybridization with 0.1 nmol/L nDNA (curve b), tmDNA (curve c), smDNA (curve d) and cDNA (curve e) and the corresponding histogram (Inset). The result shows that the R_{et} value presents negligible variation after the pDNA/Au@Bi_2S_3/GCE is hybridized with nDNA, indicating that the pDNA on the constructed biosensor could not react with nDNA and also the non-specific absorption of nDNA on Au@Bi_2S_3 does not occur. Being different, the resistance on the biosensor increases markedly, when the biosensor is incubated in cDNA solution for hybridization reaction. The phenomenon indicates that hybridized duplex DNA has been formed, and the increased steric-hindrance and electrostatic repulsion block the diffusion of $[Fe(CN)_6]^{3-/4-}$ from bulk solution to electrode surface. In addition, when the pDNA/Au@Bi_2S_3/GCE is hybridized with smDNA or tmDNA, the change of the R_{et} value is much less than the case of tDNA, but still larger than on pDNA/Au@Bi_2S_3/GCE, suggesting that only partial hybridization happens between pDNA and smDNA or tmDNA. Thus, it is concluded that the constructed biosensor has excellent hybridization selectivity to the complementary DNA from base mismatched and non-complementary DNA.

The sensitivity of the DNA biosensor is studied through incubation of the biosensor in cDNA solution with the different concentrations and comparing their EIS changes. Fig. 2B is the Nyquist plots recorded on pDNA/Au@Bi_2S_3/GCE before and after hybridization with cDNA in the concentration range from 10 fmol/L to 1 nmol/L. As shown in Fig. 2B, the R_{et} displays a steady increase with the increase of concentrations of cDNA. The R_{et} variations (ΔR_{et}) between R_{et} at the hybridized electrode and that at pDNA/Au@Bi_2S_3/GCE are well correlated to the logarithm of cDNA concentration ($\lg C_{cDNA}$) in the range from 10 fmol/L to 1 nmol/L with a regression equation of $\Delta R_{et}/(10^3\ \Omega) = 0.735$

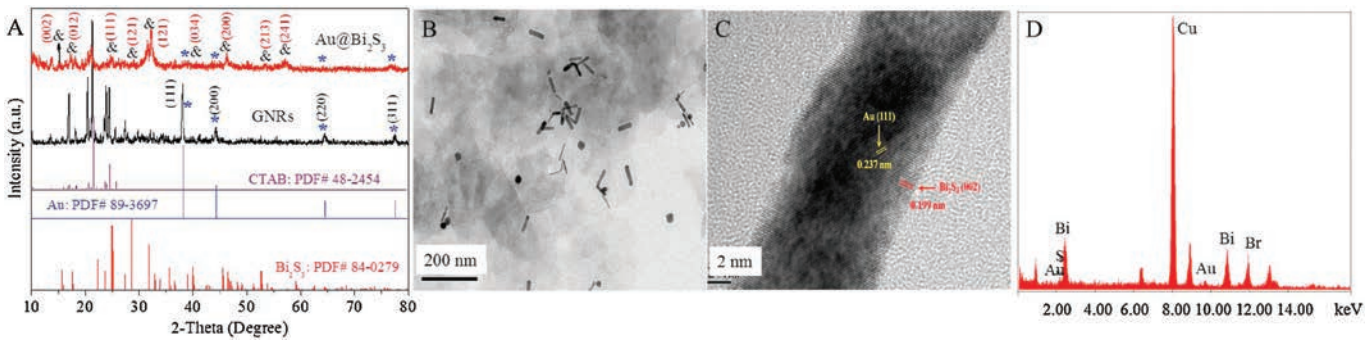

Fig. 1. XRD pattern (A), TEM (B), HRTEM (C) and EDS (D) images of the synthesized Au@Bi_2S_3.

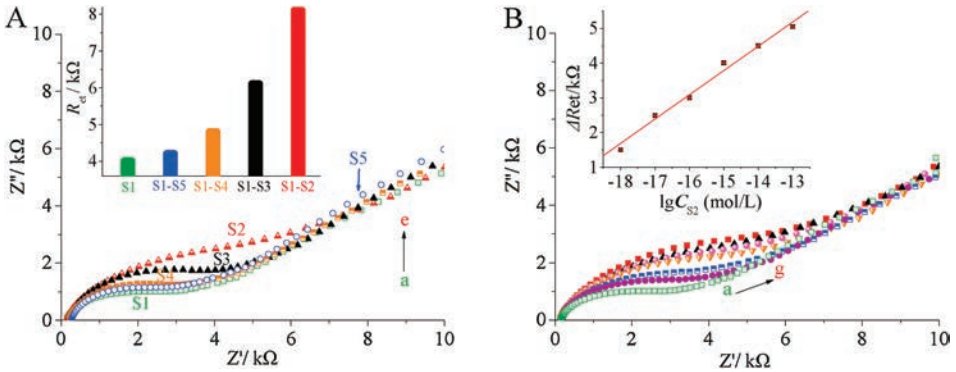

Fig. 2. (A) Nyquist plots of the biosensor (a) upon hybridization with 10 fmol/L nDNA (b), mDNA (c), smDNA (d) and cDNA (e). The inset shows the corresponding histogram. (B) Nyquist plots of the biosensor before (a) and after hybridization with 10 fmol/L (b), 100 fmol/L (c), 1 pmol/L (d), 10 pmol/L (e), 0.1 nmol/L (f), 1 nmol/L (g) cDNA. Inset is the linear plot of ΔRet values *versus* the logarithm of cDNA concentrations (lgC_{cDNA}).

lg(C_{cDNA}/M) + 14.777 (r = 0.9933) (inset of Fig. 2B). Then based on 3σ (σ was the standard deviation of a blank solution with 5 parallel measurements), the detection limit is estimated to be 2 fmol/L.

The reproducibility of the biosensor for DNA analysis was probed through hybridization of five parallel-made time pDNA/Au@Bi_2S_3/GCE with 0.1 nmol/L cDNA. When the ΔR_{et} values are adopted as analytical signal, a relative standard deviation (RSD) of 5.73% is achieved, suggesting an acceptable reproducibility of the developed pDNA/Au@Bi_2S_3/GCE for DNA analysis. In addition, the chemical stability and durability of the fabricated pDNA/Au@Bi_2S_3/GCE were investigated by storing the prepared biosensor at 4 °C for one week and hybridized with target DNA fragment. The results showed that after storage, the Au@Bi_2S_3-based biosensor showed only 3% increase of R_{et} value, indicating the excellent stability of the biosensor. When the biosensor was hybridized with 1 pmol/L cDNA, the hybridization response (ΔR_{et}) was very close to the case before storage, indicating that the developed biosensor remained the hybridization efficiency after storage, namely a good durability.

In summary, core-shell structured Au@Bi_2S_3 nanoparticles were synthesized *via* a facile seed-mediated method. Then the synthesized Au@Bi_2S_3 was further applied for fabrication of DNA biosensor. The electrochemical experimental results showed that the target DNA could be quantified in a wide concentration range from 10 fmol/L to 1 nmol/L and a low detection limit of 2 fmol/L. The high sensitivity can be explained by the synergetic effect of huge surface area and high electronic conductivity of Au@Bi_2S_3. Moreover, the sensor shows superior properties of good reproducibility, stability, and simple operation, showing that the Au@Bi_2S_3-based DNA biosensor promising to be applied in practical application.

Acknowledgments

The work is supported by the National Natural Science Foundation of China (Nos. 21802064, 21275127), Natural Science Foundation of Fujian Province, China (Nos. 2018J01435, 2017J01419), and Foundation of Key Laboratory of Sensor Analysis of Tumor Marker, Ministry of Education, Qingdao University of Science and Technology.

Appendix A. Supplementary data

Supplementary material related to this article can be found, in the online version, at doi:https://doi.org/10.1016/j.cclet.2019.04.056.

References

[1] M. Wang, H. Yin, N. Shen, et al., Biosens. Bioelectron. 53 (2014) 232–237.
[2] Q.X. Wang, F. Gao, S.X. Li, W. Weng, Z.S. Hu, Chin. Chem. Lett. 19 (2008) 585–588.
[3] Y.P. Dong, L. Huang, J. Zhang, X.F. Chu, Q.F. Zhang, Electrochim. Acta 74 (2012) 189–193.
[4] T.X. Fu, Mater. Res. Bull. 99 (2018) 460–465.
[5] X. Chen, Q. Wang, L. Wang, et al., Biosens. Bioelectron. 66 (2015) 216–223.
[6] X. Yan, Y. Gu, C. Li, et al., Sensor. Actuat. B -Chem. 257 (2018) 936–943.
[7] D.R. Kumar, S. Kesavan, M.L. Baynosa, V.Q. Nguyen, J.J. Shim, J. Colloid Interface Sci. 530 (2018) 361–371.
[8] S. Vadivel, A.N. Naveen, V.P. Kamalakannan, P. Cao, N. Balasubramanian, Appl. Surf. Sci. 351 (2015) 635–645.
[9] Q. Zhu, F. Gao, Y. Yang, et al., Sensor. Actuat. B -Chem. 207 (2015) 819–826.
[10] B. Pandit, G.K. Sharma, B.R. Sankapal, J. Colloid Interface Sci. 505 (2017) 1011–1017.
[11] S.V.P. Vattikuti, J. Shim, C. Byon, J. Solid State Chem. 258 (2018) 526–535.
[12] M. Ma, T. Zhe, W. Song, et al., Sensor. Actuat. B -Chem. 253 (2017) 818–829.
[13] S.J. Li, Y.F. Shi, L. Liu, et al., Electrochim. Acta 85 (2012) 628–635.
[14] W. Bai, H. Huang, Y. Li, et al., Electrochim. Acta 117 (2014) 322–328.
[15] M. Lin, H. Han, D. Pan, H. Zhang, Z. Su, Microchim. Acta 182 (2015) 805–813.
[16] Y. Guo, Y. Wang, G. Yang, J.J. Xu, H.Y. Chen, Biosens. Bioelectron. 85 (2016) 897–902.
[17] L. Tang, Z. Guo, X. Zheng, Sensor. Actuat. B -Chem. 279 (2019) 1–6.
[18] Y. Lai, C. Zhang, Y. Deng, et al., Chin. Chem. Lett. 30 (2019) 160–162.
[19] N. Alizadeh, A. Salimi, R. Hallaj, J. Electroanal. Chem. 811 (2018) 8–15.
[20] J. Zhang, X. Song, Z. Xiong, et al., J. Electrochem. Soc. 164 (2017) H572–H578.
[21] J. Li, H. Ma, D. Wu, et al., Biosens. Bioelectron. 74 (2015) 104–112.
[22] H. Huang, S. Huang, X. Liu, et al., Biosens. Bioelectron. 24 (2009) 3025–3029.
[23] J. Zhou, X. Li, L. Yang, et al., Anal. Chim. Acta 899 (2015) 57–65.
[24] H.H. Huang, J. Chen, Y.Z. Meng, et al., Mater. Res. Bull. 48 (2013) 3800–3804.
[25] S. Paul, S. Ghosh, D. Barman, S.K. De, Appl. Catal. B -Environ. 219 (2017) 287–300.
[26] F. Gao, X. Cai, X. Wang, et al., Sensor. Actuat. B -Chem. 186 (2013) 380–387.